

The Galaxy Pairwise Velocity Dispersion as a Function of Local Density

Michael A. Strauss¹, Jeremiah P. Ostriker, and Renyue Cen

Dept. of Astrophysical Sciences, Princeton University, Princeton, NJ 08544

ABSTRACT

The standard method of measuring the galaxy pairwise velocity dispersion on small scales via the anisotropy in the two-point correlation function in redshift space suffers from the fact that it is a *pair-weighted* statistic, and thus is heavily weighted by the densest regions in a way that is difficult to calibrate. We propose a new statistic, the redshift difference of close projected pairs of galaxies as a function of local density, which is designed to measure the small-scale velocity dispersion as an explicit function of density. Computing this statistic for a volume-limited subsample of the Optical Redshift Survey, we find that the small-scale velocity dispersion rises from 220 km s⁻¹ in the lowest density bins to 760 km s⁻¹ at high density. We calculate this statistic for a series of mock catalogs drawn from a hydrodynamic simulation of an $\Omega h = 0.5$ Cold Dark Matter universe (standard CDM), and find that the observed velocity distribution lies $\gtrsim 1\sigma$ below the simulations in each of eight density bins, formally ruling out this model at the 7.4σ level, quantifying the well-known problem that this model produces too high a velocity dispersion. This comparison is insensitive to the normalization of the power spectrum, although it is quite sensitive to the density and velocity bias of galaxies relative to dark matter on small scales.

Subject headings:

1. Introduction

The relative pair-wise velocity dispersion of galaxies σ_{12} on small ($\sim 1 h^{-1}$ Mpc) scales has long been used as a diagnostic of cosmological models. Peebles (1976a,b) used the assumption of hydrodynamic equilibrium of the galaxy population on small scales to derive the Cosmic Virial Theorem (CVT), which relates σ_{12} to the two- and three-point correlation function, and the value of the Cosmological Density Parameter Ω_0 . However, a number of authors have questioned the basic assumptions on which the CVT is based (Fisher *et al.* 1994, hereafter F94; Bartlett & Blanchard 1996; Suto & Jing 1997).

¹Alfred P. Sloan Foundation Fellow.

Davis *et al.* (1985) recognized σ_{12} as an important statistic to compare with cosmological models; indeed, the discrepancy between the predictions of the standard Cold Dark Matter model and the observed value of σ_{12} led them to adopt the then-new idea that the galaxy population is strongly biased relative to the distribution of dark matter (Bardeen *et al.* 1986). The use of σ_{12} as a distinguisher of models has been controversial ever since, and the question of the relationship between the normalization of the standard Cold Dark Matter (CDM) model and the resulting σ_{12} has been hotly debated in the literature (Ostriker & Suto 1990; Cen & Ostriker 1992; Couchman & Carlberg 1992; Gelb & Bertschinger 1994; Zurek *et al.* 1994; Brainerd & Villumsen 1994; Weinberg 1995; Brainerd *et al.* 1996; Somerville, Primack, & Nolthenius 1997).

Davis, Geller, & Huchra (1978), Peebles (1980), Davis & Peebles (1983), and Bean *et al.* (1983) introduced what is now the standard method of measuring σ_{12} . From a redshift survey of galaxies, one can measure the correlation function of galaxies in redshift space $\xi(s)$. Recognizing that peculiar velocities systematically distort the separation of pairs of galaxies along the line of sight, one can calculate ξ as a function of the component of the separation vector both parallel (π) and perpendicular (r_p) to the line of sight. In real space, the lack of a preferred direction means that $\xi(r_p, \pi)$ should be isotropic, but in redshift space, the correlations will be elongated along the π direction on small scales, because of the small-scale pairwise motions of galaxies. This effect can be modeled as a convolution of the real-space correlation of galaxies (which can be determined by a projection of $\xi(r_p, \pi)$ onto the r_p axis) with the distribution function of pairwise peculiar velocity differences, thus allowing a determination of at least the second moment of this distribution function (F94; Strauss & Willick 1995; Marzke *et al.* 1995). Recent determinations of σ_{12} from redshift survey data include F94, Marzke *et al.* (1995), and Guzzo *et al.* (1996, 1997).

However, the determination of σ_{12} by this method is quite unstable. Because it is based on the two-point correlation function, σ_{12} is pair weighted, and thus is heavily weighted by the densest regions of a sample. Because these regions naturally have the highest velocity dispersion (as one can show analytically with a straightforward extension of the CVT; Kepner, Summers, & Strauss 1997, and as we will show explicitly below), this statistic is strongly dependent on the presence or absence of rare, rich clusters within a sample (Mo, Jing, & Börner 1993; Marzke *et al.* 1995; Somerville, Davis, & Primack 1997; Guzzo *et al.* 1996, 1997). Moreover, it has been recognized for at least a decade that outside of clusters, the velocity field is very cold (Brown & Peebles 1986; Sandage 1986; Burstein 1990; Groth, Juszkiewicz, & Ostriker 1989; Ostriker & Suto 1990; Strauss, Cen, & Ostriker 1993; Willick *et al.* 1997) and it is hoped that a direct measurement of the velocity dispersion in the field would yield an even stronger constraint on cosmological models than does the global value of σ_{12} .

Indeed, the sensitivity of σ_{12} to high density, high velocity dispersion regions in both observations and simulations is the cause of much of the controversy over the comparison between models and real data referred to above. These high-density regions are intrinsically rare, and thus small observed or simulated volumes will not contain any high velocity dispersion virialized structures. Cen & Ostriker (1994) found that the rms one-dimensional velocity dispersion for

particles at $1 h^{-1}\text{Mpc}$ separation in a Mixed Dark Matter simulation increased from $\sim 400 \text{ km s}^{-1}$ to $\sim 600 \text{ km s}^{-1}$ as the box size was increased from $25 h^{-1}\text{Mpc}$ to $320 h^{-1}\text{Mpc}$, at which point it finally converged. On the observational side, this effect produces a large cosmic variance in the σ_{12} statistic (cf., Marzke *et al.* 1995). To combat this effect, some workers have omitted high density regions both from observed and simulated samples, but the results are quite sensitive to exactly how such regions are excised, and of course one is potentially throwing out valuable information in doing so.

Cen & Ostriker (1994; cf., Fig. 18b) showed from their Mixed Dark Matter simulation that the pairwise velocity dispersion is a strong function of density, smoothed on a scale of $5\text{-}10 h^{-1}\text{Mpc}$. This motivates us to develop a new measure of the pairwise velocity dispersion of galaxies from a redshift survey, *as a function of local density* (for related approaches, see Kepner *et al.* 1997; Davis, Miller, & White 1997). Although the statistic we define here is not mathematically identical to σ_{12} as conventionally defined, we show that it is a reasonable approximation. Moreover, we can calculate this statistic from Monte-Carlo realizations of our observations, drawn from simulations of various cosmological models. We can therefore use observations to compare with models, and rule them out, as the case may be.

Our primary purpose in this paper is to present our technique of measuring the velocity dispersion as a function of density. We calculate this statistic from available data, and make a preliminary comparison with the best available simulations. We introduce our statistic in § 2, and present results using the *Optical Redshift Survey* (ORS) of Santiago *et al.* (1995, 1996; hereafter S95, S96). In § 3, we compare our results to those found by applying our technique to Monte-Carlo simulations drawn from hydrodynamic and N -body simulations of various models of structure formation. Our conclusions may be found in § 4.

2. The Pairwise Velocity Dispersion as a function of Local Density

Galaxies show strong clustering on small scales. Therefore a pair of galaxies whose separation r_p on the plane of the sky is small is likely to have a small separation in real space. If the peculiar velocity difference of the pair is large relative to the real space separation expressed in velocity units, then the separation π along the line of sight is largely a measure of this peculiar velocity difference. Motivated by this simple mental picture, we will examine all pairs of galaxies whose r_p (as defined by F94) is smaller than $1 h^{-1}\text{Mpc}$. We then look at the distribution of π , the redshift space distance between these. This distribution is closely related to the correlation function along the line of sight $\int_0^1 dr_p \xi(r_p, \pi)$; indeed, it differs from this quantity only in not being normalized by the distribution expected in an unclustered universe for the given survey geometry.

We can define a local density associated with each galaxy (in redshift space) by smoothing the galaxy distribution with a Gaussian of standard deviation 400 km s^{-1} . We then simply define the density associated with any pair of galaxies as the average of the densities associated with

each one individually. The 400 km s^{-1} smoothing scale is chosen to be appreciably higher than the scale on which we examine the small-scale velocity dispersion, and large enough so that on average, several galaxies are included within the smoothing window, yet small enough that we can still refer to a *local* density field.

The following are our considerations of the appropriate data to use for this analysis:

1. The sample should be *well-defined*, to allow the local density to be determined, and to allow comparisons with results from simulations;
2. The sample should be *volume-limited*, so that the distribution of redshift differences not be a function of distance from the observer;
3. The sample should be *shallow*, to minimize the number of chance projections on the sky;
4. The sample should have *large solid angle*, to maximize the survey volume given the constraint of item 3;
5. The sample should be *dense*, to maximize the number of pairs at small separation.

The survey at our disposal that best fits these criteria is the ORS (S95, S96), and in particular, the $m = 14.5$ -limited subsample of it (ORS- m in the notation of S95). The sample covers 6.62 ster, consists of 5697 galaxies, and is drawn from three distinct galaxy catalogs in different regions of the sky. For each galaxy, we define a local density contrast δ following the techniques of S96. All calculations are done in redshift space, as measured in the rest frame of the Local Group, but for the density determination, we follow S96 in collapsing galaxies associated with several nearby clusters to a common redshift² (cf., Yahil *et al.* 1991). We then draw a volume-limited subsample to 3000 km s^{-1} , leaving 1123 galaxies. From this subsample, we identify all pairs with $r_p < 1 h^{-1} \text{ Mpc}$, and measure π , the radial component of the redshift difference vector between them.

Figure 1 is a scatter plot of the observed distribution of redshift differences of galaxy pairs as a function of local density. There is substructure in the plot, due to various discrete structures within the sample volume. In particular, the vertical stripes are due to pairs of clusters, all of whose galaxies are assigned to the same density. But the overall morphology of this plot is straightforward to understand. There is a tight core of pairs whose redshift differences are small (the horizontal concentration of points along $\pi = 0$), and whose width appears to be an increasing function of local density, and a very extended background of pairs at large separation, presumably due to the chance projections, whose distribution falls off slowly with separation. The tight core seems to disappear in the range $2 < \delta < 4$ (we will see this manifest itself in the following figure), due to the lack of clusters of the appropriate density in the relatively small volume surveyed. At

²This is of course not done in computing our redshift difference statistic!

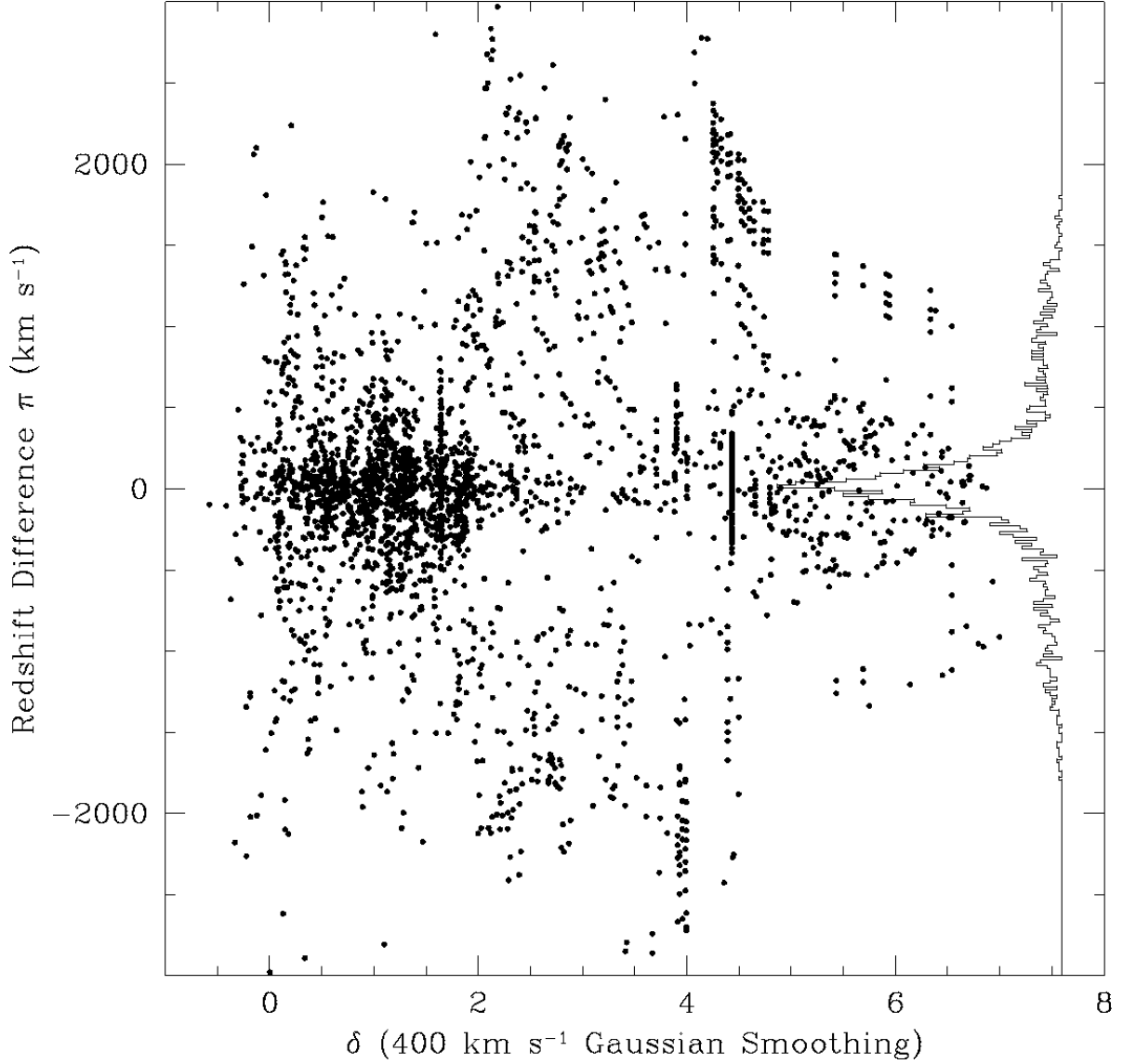


Fig. 1.— The observed distribution of differences of redshift of pairs of galaxies with projected separation less than $1 h^{-1}\text{Mpc}$, from the volume-limited subsample of the ORS. Here δ is the average overdensity of each pair in units of the sample mean density. The marginal distribution of redshift difference is shown as the histogram on the right-hand side.

very large densities, the contribution from the background disappears, because a chance projection between a cluster and field galaxy will have less than the highest possible density.

Our next step is to quantify the tightness of the central core. We do this by examining the distribution of values of π within bins of local density δ , as is shown in Figure 2. Within each bin of δ , we make a maximum likelihood fit of the observed distribution to a model of a pairwise velocity distribution plus a smooth background. Before describing the model in detail, we note that the fit is not to the binned data shown here for graphical purposes, but to the individual galaxy pairs of Figure 1.

It is argued on both empirical (F94, Marzke *et al.* 1995) and theoretical (Cen & Ostriker 1993b; Sheth 1996; Mo, Jing, & Börner 1997; Seto & Yokoyama 1997; Juszkiewicz, Fisher, & Szapudi, private communication) grounds that the distribution function of radial peculiar velocity differences between close pairs of galaxies should be exponential. Of course, the *redshift* differences of close pairs include both the effects of peculiar velocities and of true physical separation (and therefore the redshift difference distribution function can be modeled as a convolution of the correlation function with the pairwise distribution function; cf., F94), we will ignore this detail here and simply assume that the redshift difference distribution is exponential as well. This has the effect of *overestimating* the effect of the peculiar velocity dispersion (although the effect is small, as we will see); we thus will be able to put upper limits on the peculiar velocity distribution width as a function of density.

We have found empirically from Monte-Carlo tests that the background distribution is well-fit by a term proportional to $3000 \text{ km s}^{-1} - |\pi|$, therefore our model contains only two parameters:

$$f(\pi) \propto 3000 \text{ km s}^{-1} - |\pi| + A \exp\left(-\frac{2^{1/2} |\pi|}{\alpha}\right) \quad , \quad (1)$$

where A represents the relative amplitude of the central exponential relative to the background, and α is the quantity we are interested in, the second moment of the peculiar velocity distribution. The overall normalization of f is determined by the requirement that it integrate to the observed number of pairs in the density bin in question.

The results of this fit to each bin are shown as the smooth curves in Figure 2; the derived values of α are given in each panel. We could calculate formal error bars on α by finding the values at which the likelihood falls to $e^{-1/2}$ of its peak value, but the Monte-Carlo experiments we describe in the next section show this procedure underestimates the errors by factors of three or four. This is probably due to mismatch of our simplistic model with the data; in particular, the background distribution in some bins of δ clearly shows structure which our simple model does not match (cf., the bin with $3 < \delta < 5$). However, in every case, our model does do an adequate job of fitting the shape of the central peak of the observed distribution function, which is the part in which we are most interested.

As expected, the fitted distribution widths are an increasing function of density, at least

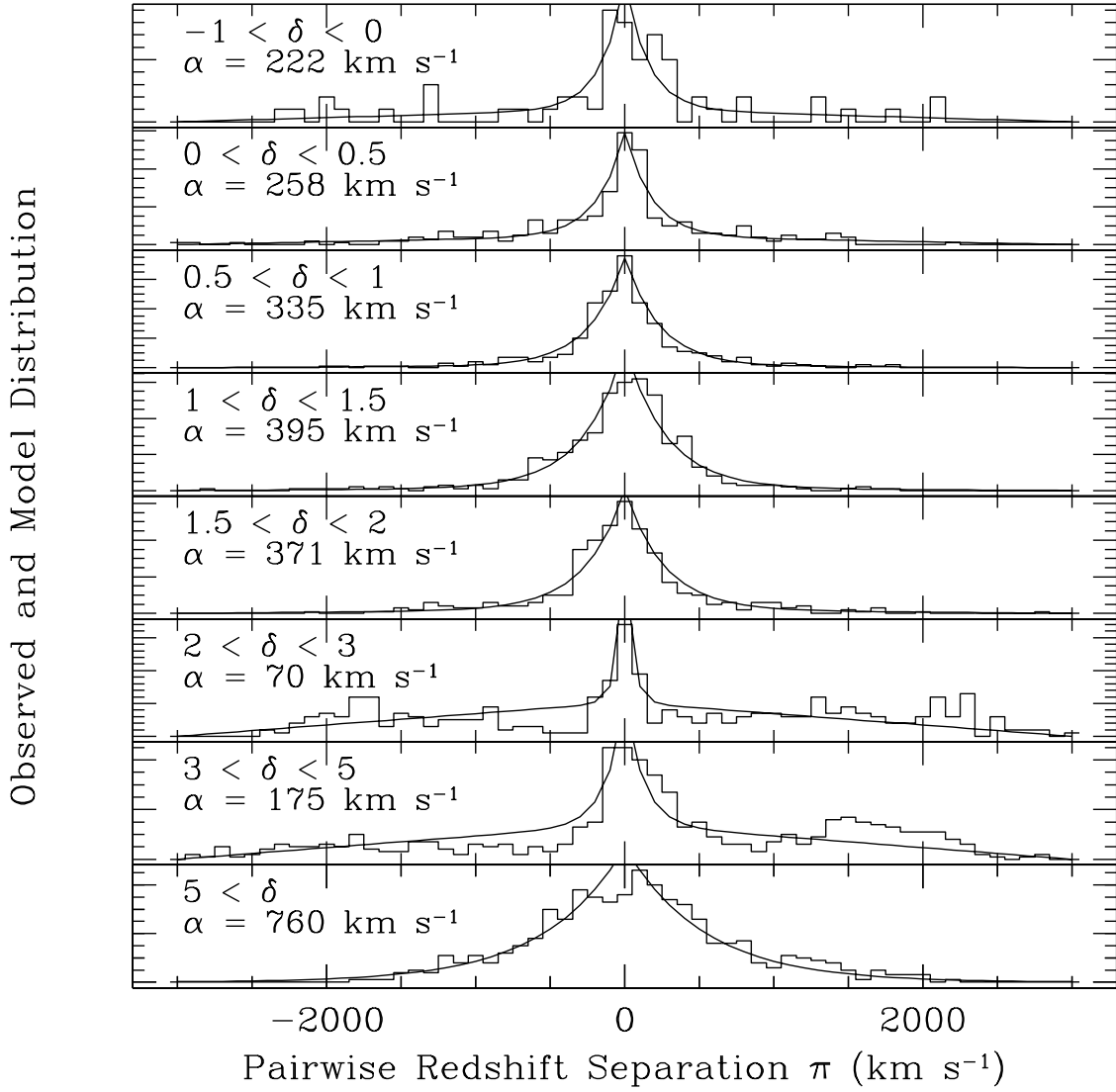


Fig. 2.— Histograms of the distribution of redshift differences π as a function of overdensity δ . The smooth curves are a maximum likelihood fit of the data in each density bin to a model of an exponential pairwise velocity distribution plus a smooth background.

to $\delta = 2$. At the next two bins, the distribution narrows; there are simply very few regions in the survey at this density, and in particular, none that are virialized with substantial velocity dispersion. This reflects the increasing cosmic variance as one examines bins of larger δ . Finally, the width in the densest bin is very large, over 500 km s^{-1} , as we would expect given that this bin mostly contains galaxies in clusters. Indeed, most of the pairs in this bin are found in the Virgo cluster, which happens to be the richest cluster within the adopted sample volume to 3000 km s^{-1} . This bin contains the largest number of galaxy pairs, which means that it carries much of the weight in standard measures of σ_{12} . If we fit the model in Eq. (1) to all the pairs of the sample (i.e., to the full distribution of Figure 1), we find a central dispersion of $\alpha = 410 \text{ km s}^{-1}$.

At low densities, the distribution of redshift differences is quite narrow, consistent with the papers quoted above of a very quiet flow field outside of clusters. The quantity whose distribution we are plotting has contributions both from peculiar velocities, and from the separation of galaxies in the radial direction in real space. We could model this formally as a convolution of the real-space correlation function with the velocity difference distribution function, *if we knew how to calculate the real space correlation function for the subset of those galaxies in a given local density range*. We will see in the next section that this effect is small; α as we measure it is in fact a decent approximation to the true small-scale peculiar velocity dispersion.

3. Comparisons with Simulations

In this section, we use hydrodynamic and N -body cosmological simulations for two purposes. We first compare the results of our redshift difference statistic to the right answer, which we know *a priori* for the simulations. After demonstrating that the redshift difference statistic is indeed measuring something close to the true small-scale velocity dispersion of galaxies, we can further use the simulations to compare our observed results with models.

On the $1\text{-}2h^{-1}\text{Mpc}$ scales we are considering here, the small-scale clustering and peculiar velocity properties of galaxies will be greatly affected by the details of one’s model for the relative distribution of galaxies and dark matter. In this highly non-linear regime (in the sense that $\langle \delta^2 \rangle \gg 1$), the simple *ansatz* of linear biasing ($\delta_{\text{galaxies}} = b \delta_{\text{dark matter}}$) cannot be expected to hold, nor can we presume that the velocity fields of galaxies and dark matter trace one another (velocity bias; cf., Carlberg, Couchman, & Thomas 1990; Cen & Ostriker 1992). We therefore need simulations that include enough of the relevant physics to allow us to identify galaxies. Here we use the Standard CDM (SCDM) hydrodynamic simulation of Cen & Ostriker (1992, 1993ab), which simulated a cube $80h^{-1}\text{Mpc}$ on a side with 200^3 particles and 200^3 cells. The parameters of the input power spectrum are given in Table 1.

We identify galaxies as follows (Cen & Ostriker 1992): At each time step, we consider those cells with baryonic overdensity ($\delta\rho/\rho$) > 5.5 as candidates for regions within which galaxy formation will occur. If a cell also satisfies the following criteria: the region is collapsing in real

coordinates, the cooling time is less than its dynamical time, and the baryonic mass is larger than the Jean mass for its density and temperature, the gas must collapse towards the center of the cell with subsequent condensation into a stellar system. So we remove from the gas in the cell in question the mass that would collapse in timestep Δt and create a collisionless particle at the center of the cell, giving it the same proper velocity as the gas in the cell. After creation, these new particles are treated dynamically as dark matter particles. The three components (gas, galaxies and dark matter) interact through gravity. At any epoch of interest we construct the galaxies out of the collisionless sub-units formed in cooling collapsing regions using an adaptive, friends-of-friends linking scheme (Suto, Cen & Ostriker 1992) to join together neighboring particles into galactic units with the linking parameters chosen such that the galaxy mass function fits observations (Cen & Ostriker 1993b).

Given this galaxy list, we are ready to make a simulated redshift survey. We choose a candidate to represent the Local Group as we have done in previous papers (e.g., Strauss *et al.* 1992, 1993): the galaxy must have a peculiar velocity in the range 520 to 720 km s⁻¹, and have a local density δ between -0.2 and 1. We then select galaxies, with mass greater than $10^{9.8} M_{\odot}$, within a sphere of radius 3000 km s⁻¹ around it, at the number density appropriate for each region in the ORS. The ORS excluded zones (especially the zone of avoidance) are put in, and the effects of extinction on the galaxy number density is also included, using the Burstein-Heiles (1982) extinction maps. We calculate the 400 km s⁻¹ Gaussian smoothed density field around each mock galaxy in redshift space, first collapsing conspicuous clusters as we did in the real universe. The resulting galaxy catalog is then put into the identical code used above to calculate the velocity dispersion statistic, and the results are tabulated. One hundred mock realizations of the ORS sample are generated.

For the simulation, we of course know the true peculiar velocity of every galaxy, and therefore we can compare the true difference in peculiar velocity, Δv_p for every pair with projected separation $< 1 h^{-1}$ Mpc, to the redshift difference π . This comparison is shown in the upper-left panel of Figure 3. For pairs with projected separation this small, the redshift-space difference is indeed an impressively good measure of the peculiar velocity difference of galaxies. The difference $\pi - \Delta v_p$ is shown in the upper right panel, as a function of local density. The vast majority of the points form a tight core with a dispersion less than 100 km s⁻¹. The background is more severe at low densities; chance projections are more important there, as our intuition would tell us. This forms the background that we take out in the model of equation (1).

For any Monte-Carlo realization of the ORS sample, we can directly calculate the standard deviation σ of peculiar velocity differences of the close galaxy pairs chosen in a given density bin, and compare it directly to the value derived from the distribution of π . This comparison is made in the lower-left panel for the 100 mock realizations, at each value of density. The agreement between the two quantities is excellent. The lower-right panel shows the fractional difference between α and σ as a function of local density. The derived velocity dispersion is slightly biased upwards (as we would expect, given the argument at the end of the previous section) by a mean

of 30% at low densities, and appreciably less at high densities. The scatter is impressively small, especially at high densities.

Thus despite the contamination from projected pairs of galaxies, and the nonuniform sampling of the ORS, the quantity α measured from the distribution of redshift differences is a good measure of the small-scale velocity dispersion of galaxies. With this assurance in mind, we make a direct comparison between the observations and simulations in Figure 4. The open points are the observed values of α as a function of local density for the real ORS sample. The small points are the results from each of the 100 Monte-Carlo mock realizations of the ORS data, with a small scatter added to the ordinate to make them easier to distinguish. Thus the open circles (data) and the small dots (simulation) may be compared directly. The mean and standard deviation over the realizations at each δ are given by the large solid points with their errors³. The data lie roughly one standard deviation below the simulations in almost all density bins, the exception, interestingly enough, being the highest density bin. The formal χ^2 difference between the observations and the model is 80.5 for 8 degrees of freedom, assuming Gaussian errors and no covariance between bins; not surprisingly, this is dominated by the points at $\delta = 3$ and $\delta = 4$. Formally, this rules out the SCDM model at the 7.4σ level. Of course, the χ^2 statistic does not reflect the fact that the data lies systematically *lower* than the model in all density bins. Thus the well-established fact that the standard CDM model over-predicts the observed small-scale velocity dispersion is not just a reflection of a mismatch at cluster cores; it extends to the lowest density regions.

What is it about the standard CDM model that causes it to miss the observed velocity dispersion so dramatically? The normalization of the power spectrum in this simulation is roughly 35% below the COBE normalization of Bunn & White (1997) (cf., the discussion in Cen & Ostriker 1993b), and was chosen to provide a fit to various observed phenomena at the several Mpc scale. We wish to test the sensitivity of the velocity dispersion statistic to this normalization. Rather than repeat the simulation with a different normalization, we note that the amplitude grows with time, and so we simply look at this simulation at an earlier epoch. Thus, we calculate the one-dimensional velocity dispersion σ of dark matter particles separated by $< 1 h^{-1}\text{Mpc}$ from the CDM simulation at $z = 0$, $z = 0.5$, and $z = 0.7$. Here we measure this statistic directly from the simulation, and do not make Monte-Carlo redshift survey realizations. For this $\Omega = 1$ simulation, the linear amplitude of fluctuations is down by factors of 0.67 and 0.59, respectively, relative to the amplitude at $z = 0$. Figure 5a shows the velocity dispersion as a function of local density. At higher redshifts, the dynamic range of densities is smaller than that at lower redshifts, of course, but at a given overdensity, the velocity dispersion is unchanged. Therefore, the mismatch between the observed and predicted peculiar velocity dispersions as a function of density in the standard CDM model cannot be fixed by changing the normalization of the model (cf., the discussion in Kepner *et al.* 1997). Note that this is not the case for the small-scale velocity dispersion averaged over density, as traditionally defined; indeed, Davis *et al.* (1985) used the observed small-scale

³These error bars are typically three times larger than the formal errors of the model fit.

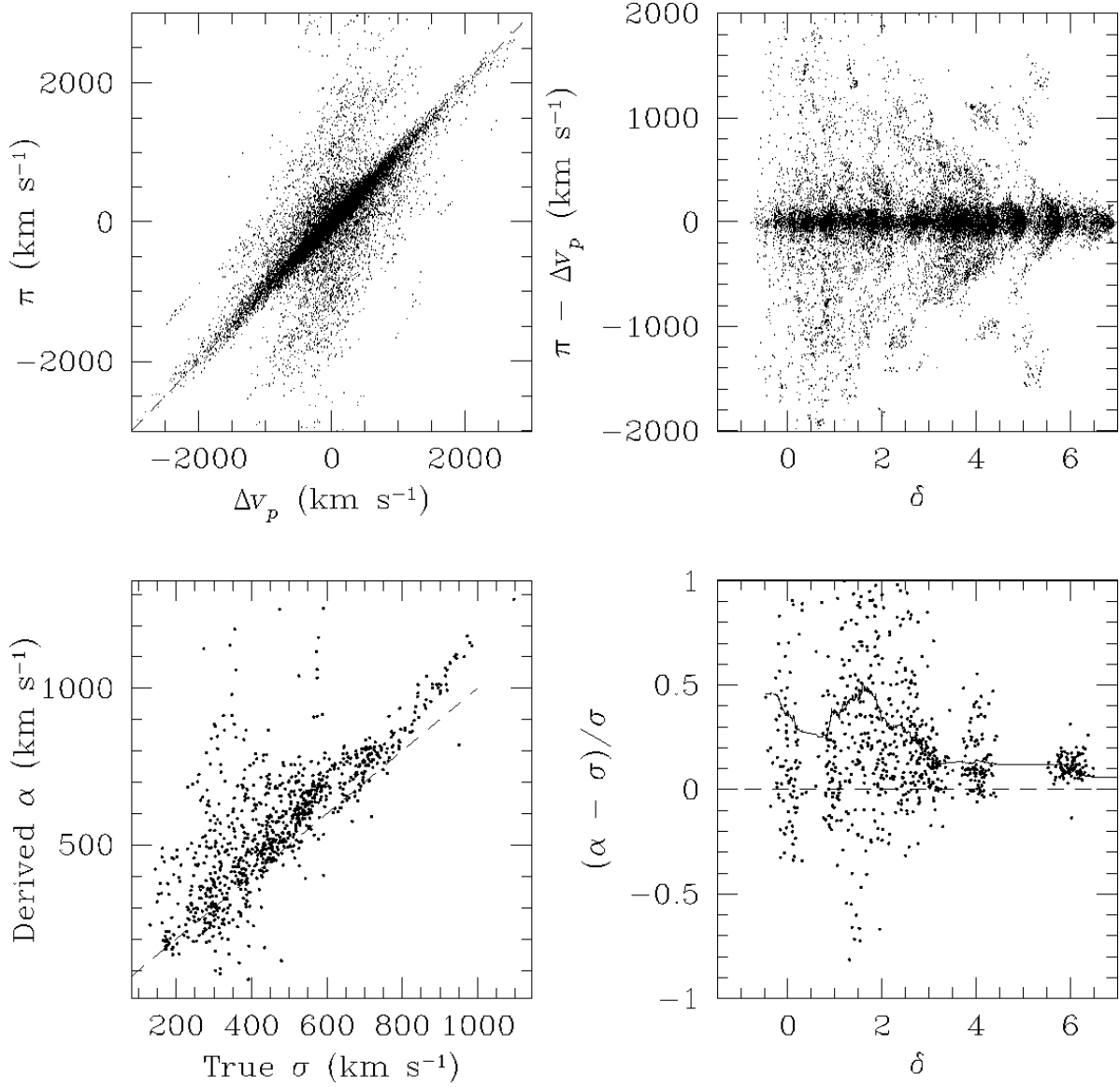


Fig. 3.— Comparisons of those statistics measured in redshift space with the truth, for 100 mock realizations of the ORS sample drawn from a hydrodynamic simulation of galaxies in a standard CDM universe. Upper left panel: the comparison between Δv_p , the true peculiar velocity difference of pairs of galaxies with projected separation $< 1 h^{-1} \text{Mpc}$, with their redshift-space difference, π . Upper right panel: the difference $\pi - \Delta v_p$ as a function of local density, as determined from a 400 km s^{-1} Gaussian smoothing. Lower left panel: the comparison between the scale-length α of the redshift-space difference of pairs of galaxies, with the standard deviation σ of their true peculiar velocity difference. For each realization, results are shown at a variety of local densities. Lower right panel: the fractional difference between these two quantities as a function of local density. A small scatter has been added to the ordinate in this plot to make it easier to read. The running mean is given by the thin solid line.

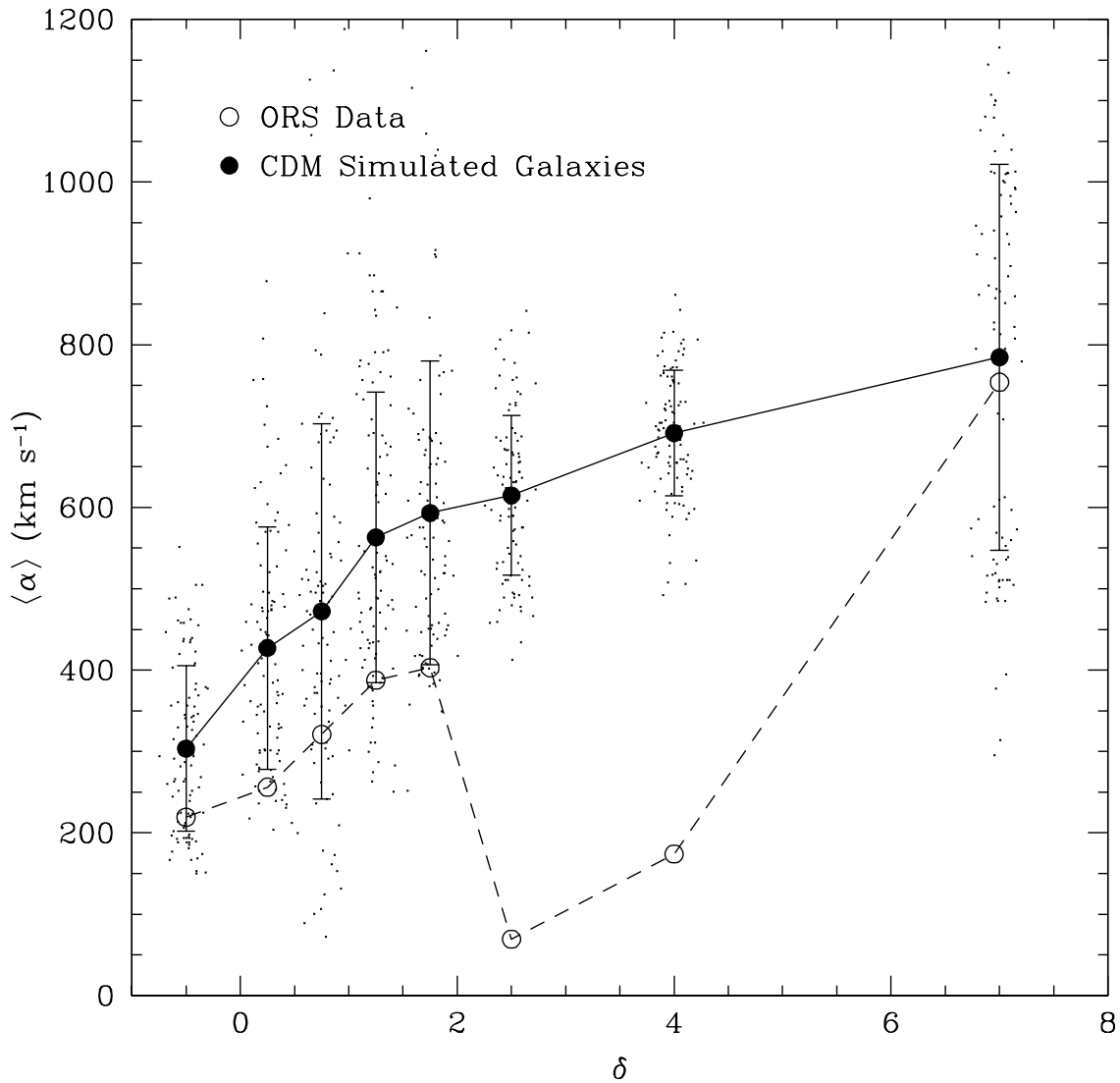


Fig. 4.— The open points show the observed velocity dispersion statistic α as a function of local overdensity, for the real ORS sample. The small points are the results of 100 individual Monte-Carlo mock realizations of the full ORS sample, drawn from a hydrodynamic simulation of galaxies in a standard Cold Dark Matter universe. The solid points with error bars are the mean and standard deviation over these realizations in each density bin.

velocity dispersion to set the bias of the Standard CDM model to $b = 2.5$ (equivalently, $\sigma_8 \approx 0.4$).

Large-scale hydrodynamic simulations with galaxy formation at the level of sophistication of that used above are quite time-consuming to carry out, and we only have the single SCDM model at our disposal for the comparison with observations. We argued above that simulations which include galaxy formation are necessary to compare to observations, given our lack of knowledge of the nature of biasing on small scales. Nevertheless, it is interesting to ask how the velocity dispersion as a function of density of galaxies is related to that of dark matter. Figure 5b compares the one-dimensional velocity dispersion as a function of density for galaxies and dark matter, from the standard CDM simulation. There are two physical effects which cause the two to differ: density bias, which causes changes in the abscissa of the graph, and velocity bias, which causes changes to the ordinate. One can measure these two effects directly from the simulation itself (Cen & Ostriker 1992). At our density smoothing scale, the density bias is roughly 1.6; that is: $\delta_{\text{galaxies}} = 1.6 \delta_{\text{dark matter}}$. The velocity dispersion on small scales of galaxies is $\sim 80\%$ that of the dark matter (velocity bias; cf., the discussion in Carlberg *et al.* 1990; Cen & Ostriker 1993b; Carlberg 1994; Summers, Davis, & Evrard 1995). Rescaling the two axes of the graph by these factors for the dark matter gives Figure 5c. The two curves are now in qualitative agreement, telling us that at least to first order, the difference in the velocity dispersion as a function of local density between galaxies and dark matter in the simulations can be understood in terms of linear velocity and density bias.

We now use dark matter N -body simulations of a variety of power spectra to examine the dependence of the velocity dispersion-overdensity relation on cosmological model. These will not be useful to compare with observations, given our lack of understanding of the velocity and density bias in each of these models, but they do show how strongly the velocity dispersion statistic can distinguish between models in principle. The dark matter simulations are done in a $128 h^{-1}\text{Mpc}$ box with a 720^3 PM grid and 240^3 particles. The particle mass is $4.2 \times 10^{10} \Omega_0 h^{-1} M_\odot$ and the spatial resolution is $0.44 h^{-1}\text{Mpc}$ (~ 2.5 grid cells), both adequate for our purposes. The details of the power spectra assumed are given in Table 1. Figure 6 shows the resulting velocity dispersion as function of overdensity.

Some of the results can be understood intuitively. The velocity dispersion of the HDM model in the high-density nonlinear caustics is very high, but in the low-density regions, no nonlinear structures have formed, and thus the effective power spectrum on small scales is very small. Thus the velocity dispersion becomes vanishingly small at low densities, in disagreement with what is observed (Figure 4). The two low Ω_0 CDM models differ only in the presence or absence of a cosmological constant; this makes essentially no difference to their dynamics today (cf., Lahav *et al.* 1991). With lower Ω_0 , the CVT says that these models have appreciably smaller small-scale velocity dispersion than does the standard CDM model, bringing them into better agreement with the observations (compare these curves with that in Figure 4). Finally, the $P(k) \propto k^{-2}$ model has less small-scale power, and therefore a smaller velocity dispersion, than does the $P(k) \propto k^{-1}$ model. These models have a smaller fraction of their volume at low density than do the others,

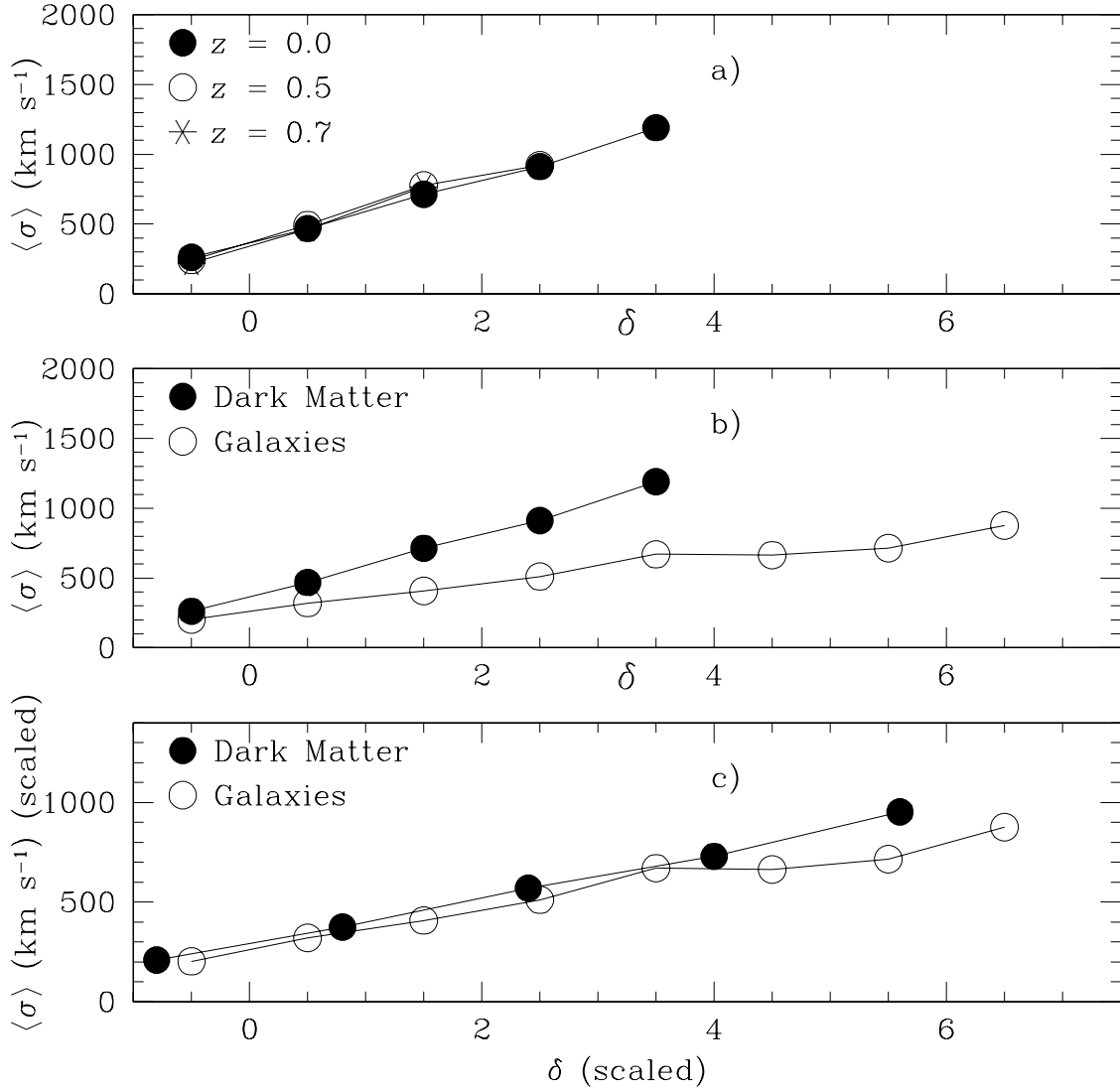


Fig. 5.— a. The one-dimensional velocity dispersion on $1 h^{-1}$ Mpc scales as a function of local density for N -body points from simulations of a standard CDM universe, at three different redshifts. b. The dark matter velocity dispersion as a function of dark matter density at $z = 0$, compared with the velocity dispersion of galaxies from the same simulation, as a function of the galaxy density. c. As in (b), but with the dark matter density and velocity dispersion scaled for a density bias $b = 1.6$ and a velocity bias of 80%.

and thus the velocity dispersion is systematically higher. Note that as we would expect from the CVT (cf., Kepner *et al.* 1997), all $\Omega_0 = 1$ models have similar velocity dispersions at high densities; they are ordered roughly by the value of the rms mass fluctuations on $1 h^{-1}\text{Mpc}$ scales in each model.

Figure 6 shows results for dark matter particles; as discussed above, we need a model for density and velocity bias of galaxies in each model in order to compare with observations. We would expect *a priori* that the density bias should be smaller in the low Ω_0 CDM models than in the SCDM model, from two arguments. First, as emphasized by Chiu, Ostriker, & Strauss (1997), the abundance of rich clusters and comparisons of the galaxy density and velocity fields constrain the quantity $\Omega_0^{0.6}/b$; thus the low- Ω_0 models should have lower bias. Second, in a low- Ω_0 universe, structure freezes out at high redshift, and thus the baryons have an extended period in which to fall into the dark potential wells. Therefore, at the present, we expect the baryons to have “caught up”, and thus show a value of b close to unity (cf., Fry 1996). Similarly, we would expect the velocity bias to be smaller as well. The scaling arguments of Figure 5 show that the SCDM, OCDM, and LCDM *galaxy* velocity dispersion as function of *galaxy* density may thus be more similar to one another than Figure 6 would imply. It would be amusing indeed if they become degenerate, but it will require full galaxy formation simulations of the low- Ω_0 models to determine if this is indeed the case.

4. Discussion and Conclusions

We have developed and tested a method to measure the small-scale velocity dispersion of galaxies from a redshift survey, as a function of local density. This approach is much less sensitive to the presence or absence of a rich cluster in the survey volume than is the traditional velocity dispersion of galaxies. As expected, the observed velocity dispersion of galaxies is an increasing function of local density, varying between 220 km s^{-1} at low densities, to 760 km s^{-1} at high densities. The small value of the velocity dispersion at low densities is consistent with reports of a cold velocity flow of galaxies outside of clusters. For example, Willick *et al.* (1997) report from an analysis of Tully-Fisher data that the pairwise velocity dispersion of spiral galaxies of $175 \pm 30 \text{ km s}^{-1}$, in good agreement with our value at low densities. Davis *et al.* (1997) find a pairwise velocity dispersion of *IRAS* galaxies of $140 \pm 22 \text{ km s}^{-1}$ in their single-particle-weighting technique, which is well *below* our value; their value for optically selected galaxies, $180 \pm 22 \text{ km s}^{-1}$, is in good agreement with ours.

We have found that the long-standing discrepancy between observed small-scale velocity dispersion of galaxies, and the predictions of the standard CDM model with COBE-normalization, is apparent even when plotted as a function of local density. Thus the problem cannot be “solved” by restricting attention to any particular regime of overdensity.

This did not have to be the case; it is well-known that the abundance of rich clusters in

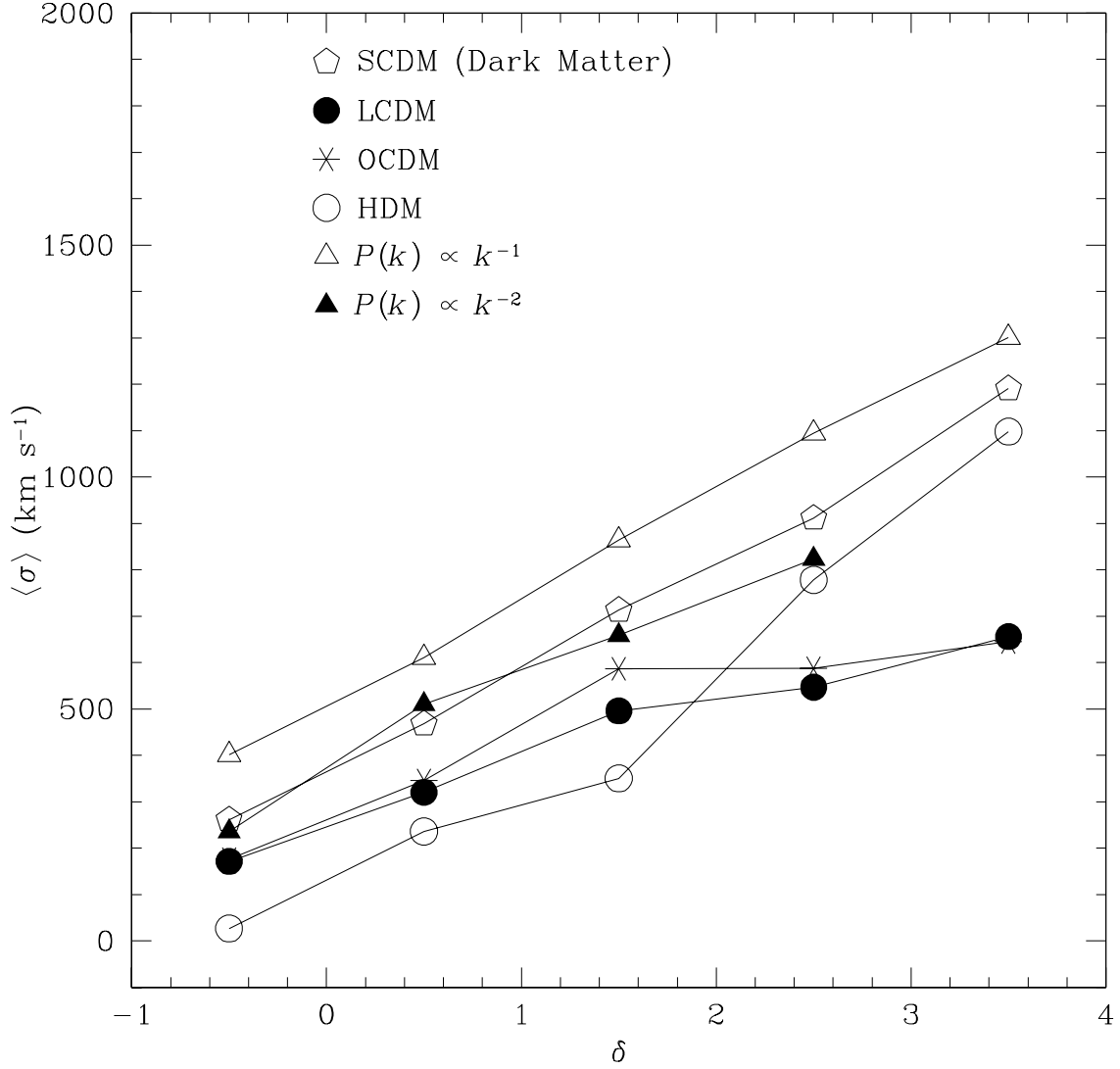


Fig. 6.— The one-dimensional pairwise velocity dispersion on $1 h^{-1}\text{Mpc}$ scales as a function of local density for N -body points from simulations of a series of different cosmological models. The SCDM points are from dark matter points in the SCDM hydrodynamic simulation.

standard CDM is appreciably larger than the observed value (e.g., Bahcall & Cen 1992); this is closely related to the fact that the observed abundance of clusters puts a tight constraint on the combination $\sigma_8\Omega^{0.56}$ (cf., White, Efstathiou, & Frenk 1993; Eke, Cole & Frenk 1996; Viana & Liddle 1996; Pen 1996; Fan, Bahcall, & Cen 1997; Chiu *et al.* 1997), giving a value about half that appropriate for COBE-normalized standard CDM (a problem that *can* be addressed by altering the normalization). As we argued in the introduction, the standard velocity dispersion statistic is heavily weighted by clusters, meaning that if a model overpredicts the distribution of clusters, it is bound to overpredict the galaxy velocity dispersion. Plotting the velocity dispersion as a function of local density removes this problem, and yet the standard CDM model still overpredicts the observed velocity dispersion, even at low densities. Our Monte-Carlo experiments show that in any single bin of density, the observations do not rule out SCDM at an interesting level, but the velocity dispersion is overpredicted consistently by the model in all bins. If we treat the distribution of values in the simulations as Gaussian, and the different bins as independent, we formally rule out CDM at the 7.4σ significance level.

The predicted velocity dispersion as a function of density is quite insensitive to the normalization of the power spectrum. The small-scale velocity dispersion as a function of local density is quite different when calculated from dark matter particles and galaxies in a hydrodynamic simulation; this may be understood to first order as due to a combination of density and velocity bias. We need sophisticated galaxy-forming hydrodynamic simulations of a series of models in order to make further comparisons of observations with models. However, rough comparisons with N -body simulations suggests that the HDM model cannot match the observed velocity dispersion, while low- Ω_0 CDM models should fare better than standard CDM. We are in the process of running hydrodynamic simulations with roughly three times the spatial resolution, nine times the mass resolution, and improved cooling models for a variant of the LCDM model; we look forward to measuring the velocity dispersion as a function of overdensity for this simulation, and comparing with observations.

The ORS is the best available redshift survey for calculating the velocity dispersion statistic. The *IRAS* 1.2 Jy survey (Fisher *et al.* 1995) is too sparse to give an interesting number of pairs at small separation. It is possible that the *IRAS* 0.6 Jy survey (the PSC-z; cf, Efstathiou 1997) will be well-suited for our statistic. In the future, we could imagine using a volume-limited subsample from the Sloan Digital Sky Survey (cf., Gunn & Weinberg 1995; Strauss 1997) 3000 km s^{-1} thick at $\sim 30,000 \text{ km s}^{-1}$ from the Local Group, containing of the order of 60,000 galaxies. This would allow us to measure this statistic to much higher accuracy over a substantially larger volume.

M.A.S. acknowledges the support of the Alfred P. Sloan Foundation, NASA Theory Grant NAG5-2882, NSF Grant AST96-16901 and the hospitality of the Astronomy Department of the University of Tōkyō, where much of this work was carried out. J.P.O. and R.C. were supported by NASA grant NAG5-2759 and NSF Grant ASC93-018185. We thank Ofer Lahav, Basilio Santiago, Alan Dressler, Marc Davis, and John Huchra (the ORS team) for permission to use the ORS data

before publication.

REFERENCES

- Bahcall, N. A., & Cen, R. 1992, ApJ, 398, L81
- Bardeen, J., Bond, J. R., Kaiser, N., & Szalay, A. 1986, ApJ, 304, 15
- Bartlett, J. G. & Blanchard, A. 1996, A&A, 307, 1
- Bean, A. J., Efstathiou, G. P., Ellis, R. S., Peterson, B. A., & Shanks, T. 1983, MNRAS, 205, 605
- Brainerd, T. G., Bromley, B. C., Warren, M. S., & Zurek, W. 1996, ApJ, 464, L103
- Brainerd, T. G. & Villumsen, J. V. 1994, ApJ, 436, 528
- Brown, M. E., & Peebles, P. J. E. 1987, ApJ, 317, 588
- Bunn, E. F., & White, M. 1997, 480, 6
- Burstein, D. 1990, Rep. Prog. Phys., 53, 421
- Burstein, D., & Heiles, C. 1982, AJ, 87, 1165
- Carlberg, R. G. 1994, ApJ, 433, 468
- Carlberg, R. G., Couchman, H. M. P., & Thomas, P. A. 1990, ApJ, 352, L29
- Cen, R., & Ostriker, J. P. 1992, ApJ, 399, L113
- Cen, R., & Ostriker, J. P. 1993a, ApJ, 417, 404
- Cen, R., & Ostriker, J. P. 1993b, ApJ, 417, 415
- Cen, R., & Ostriker, J. P. 1994, ApJ, 431, 451
- Chiu, W., Ostriker, J. P., & Strauss, M. A. 1997, in preparation
- Couchman, H. M. P., & Carlberg, R. G. 1992, ApJ, 389, 453
- Davis, M., Efstathiou, G., Frenk, C. S., & White, S. D. M. 1985, ApJ, 292, 371
- Davis, M., Geller, M. J, & Huchra, J. 1978, ApJ, 221, 1
- Davis, M., Miller, A., & White, S. D. M. 1997, ApJ, in press (astro-ph/9705224)
- Davis, M., & Peebles, P. J. E. 1983, ApJ, 267, 465
- Efstathiou, G. P. 1997, in *Critical Dialogues in Cosmology*, edited by N. Turok (Singapore: World Scientific), in press
- Eke, V. R., Cole, S., & Frenk, C. S. 1996, MNRAS, 282, 263
- Fan, X., Bahcall, N., & Cen, R. 1997, ApJ, submitted
- Fisher, K. B., Davis, M., Strauss, M. A., Yahil, A., & Huchra, J. P. 1994, MNRAS, 267, 927 (F94)
- Fisher, K. B., Huchra, J. P., Strauss, M. A., Davis, M., Yahil, A., & Schlegel, D. 1995, ApJS, 100, 69

- Fry, J.N. 1996, ApJ, 461, L65
- Gelb, J. M., & Bertschinger, E. 1994, ApJ, 436, 491
- Groth, E. J., Juskiewicz, R., & Ostriker, J. P. 1989, ApJ, 346, 558
- Gunn, J. E., & Weinberg, D. H. 1995, in *Wide-Field Spectroscopy and the Distant Universe*, ed. S. J. Maddox and A. Aragón-Salamanca (Singapore: World Scientific), 3
- Guzzo, L., Fisher, K. B., Strauss, M. A., Giovanelli, R., & Haynes, M. P. 1996, *Astrophysics Letters and Communications*, 33, 231
- Guzzo, L., Strauss, M. A., Fisher, K. B., Giovanelli, R., & Haynes, M. P. 1997, ApJ, 489, in press (astro-ph/9706150)
- Kepner, J. V., Summers, F. J., & Strauss, M. A. 1997, *New Astronomy*, 2, 165
- Lahav, O., Lilje, P. B., Primack, J. R., & Rees, M. J. 1991, MNRAS, 251, 128
- Marzke, R. O., Geller, M. J., da Costa, L. N., & Huchra, J. P. 1995, AJ, 110, 477
- Mo, H. J., Jing, Y. P., & Börner, G. 1993, MNRAS, 264, 825
- Mo, H. J., Jing, Y. P., & Börner, G. 1997, MNRAS, 286, 979
- Ostriker, J. P., & Suto, Y. 1990, ApJ, 348, 378
- Peebles, P. J. E. 1976a, A&A, 53, 131
- Peebles, P. J. E. 1976b, ApJ, 205, L109
- Peebles, P. J. E. 1980, *The Large Scale Structure of the Universe* (Princeton: Princeton University Press)
- Pen, U. -L. 1996, preprint (astro-ph/9610147)
- Sandage, A. 1986, ApJ, 307, 1
- Santiago, B. X., Strauss, M. A., Lahav, O., Davis, M., Dressler, A., & Huchra, J. P. 1995, ApJ, 446, 457 (S95)
- Santiago, B. X., Strauss, M. A., Lahav, O., Davis, M., Dressler, A., & Huchra, J. P. 1996, ApJ, 461, 38 (S96)
- Seto, N., & Yokoyama, J. 1997, preprint
- Sheth, R. K. 1996, MNRAS, 279, 1310
- Somerville, R. S., Davis, M., & Primack, J. R. 1997, ApJ, 479, 616
- Somerville, R. S., Primack, J. R., & Nolthenius, R. 1997, ApJ, 479, 606
- Strauss, M. A. 1997, *Redshift Surveys of the Local Universe*, in *Formation of Structure in the Universe*, edited by Avishai Dekel and Jeremiah P. Ostriker (Cambridge: Cambridge University Press), in press
- Strauss, M. A., Cen, R., & Ostriker, J. P. 1993, ApJ, 408, 389

- Strauss, M. A., & Willick, J. A. 1995, *Physics Reports*, 261, 271
- Strauss, M. A., Yahil, A., Davis, M., Huchra, J. P., & Fisher, K. B. 1992, *ApJ*, 397, 395
- Summers, F. J., Davis, M., & Evrard, A. 1995, *ApJ*, 451, 1
- Suto, Y., Cen, R., & Ostriker, J.P. 1992, *ApJ*, 395, 1
- Suto, Y., & Jing, Y. -P. 1997, *ApJS*, 110, 167
- Viana, P. T. P., & Liddle, A. R. 1996, *MNRAS*, 281, 323
- Weinberg, D. H. 1995, in *Wide-Field Spectroscopy and the Distant Universe*, eds. S. J. Maddox and A. Aragón-Salamanca (Singapore: World Scientific), 129
- White, S. D. M., Efstathiou, G., & Frenk, C. S. 1993, *MNRAS*, 262, 1023
- Willick, J. A., Strauss, M. A., Dekel, A., & Kolatt, T. 1997, *ApJ*, 486, in press (astro-ph/9612240)
- Yahil, A., Strauss, M. A., Davis, M., & Huchra, J. P. 1991, *ApJ*, 372, 380
- Zurek, W. H., Quinn, P. J., Salmon, J. K., & Warren, M. S. 1994, *ApJ*, 431, 559

Table 1. Simulations Used

Model	Ω_0	Λ	h	σ_8	Boxsize	Comments
SCDM	1.00	0.0	0.50	0.77	$80 h^{-1}\text{Mpc}$	Hydro simulation, $\Omega_b = 0.06$
LCDM	0.40	0.6	0.65	0.79	$128 h^{-1}\text{Mpc}$	N -body simulation; Cold Dark Matter
OCDM	0.35	0.0	0.70	0.80	$128 h^{-1}\text{Mpc}$	N -body simulation; Cold Dark Matter
HDM	1.00	0.0	0.50	1.05	$128 h^{-1}\text{Mpc}$	N -body simulation; Hot Dark Matter
POW1	1.00	0.0	0.50	1.05	$128 h^{-1}\text{Mpc}$	N -body simulation; $P(k) \propto k^{-1}$
POW2	1.00	0.0	0.50	1.05	$128 h^{-1}\text{Mpc}$	N -body simulation; $P(k) \propto k^{-2}$